

Matrix Isolation Infrared and *ab Initio* Study of the 1:1 Complexes of Cyclopentadiene with Nitrogen and Oxygen Bases: C–H···N(O) Hydrogen Bonding Involving an sp^3 -Hybridized Carbon

Mark A. Hilfiker, Erin R. Mysak, and Cindy Samet*

Department of Chemistry, Dickinson College, Carlisle, Pennsylvania 17013

Andy Maynard

Laboratory of Experimental and Computational Biology, IRSP, SAIC–Frederick, National Cancer Institute–FCRDC, Frederick, Maryland 21702

Received: December 11, 2000

Hydrogen-bonded complexes of cyclopentadiene with the strong bases ammonia, trimethylamine, and dimethyl ether have been isolated and characterized for the first time in argon matrices at 16 K. Coordination of the acidic alkyl hydrogen to the electron donor was evidenced by distinct red shifts of the CH_2 stretching modes of cyclopentadiene in the infrared spectrum. An additional $NH\cdots\pi$ interaction was evidenced by the red shift of an olefinic C–H stretching mode. *Ab initio* calculations yield a complex with NH_3 located above the ring, oriented by both of these hydrogen-bonding interactions. The calculated interaction energy of the complex is 2.40 kcal/mol, with the energy being divided equally between these two interactions. This study represents the first example of an sp^3 -hybridized carbon on a hydrocarbon taking part in a C–H···N(O) hydrogen bond.

Introduction

The concept of the hydrogen bond is important to numerous phenomena that lie at the interface of chemistry, biology, and physics.¹ In molecular recognition,² for example, a receptor must be strong enough to hold a neurotransmitter yet weak enough to let go quickly once the message is delivered. Weak hydrogen bonds can facilitate this task, and the late Linus Pauling recognized early³ that these “velcro” bonds would be important to biological chemistry. Although experimental and theoretical studies of hydrogen bonds are being pursued in many laboratories, few of these studies involve the characterization of weak hydrogen bonds. In particular, little is known about the way in which C–H bonds of hydrocarbons interact to form hydrogen bonds with electron donors. Since hydrogen bonds typically form with the electronegative elements N, O, and F, studies involving nitrogen and oxygen bases are useful. Characterization of the C–H···O and C–H···N hydrogen bond is important to the modeling of hydrophilic interactions in solution and to an understanding of the structure of organic crystals.⁴ There are abundant examples in the recent literature of C–H···O hydrogen bonds stabilizing supramolecular assemblies and therefore playing a part in crystal engineering,⁵ cluster-based organometallic chemistry,⁶ and macrocyclization processes.⁷ Recently, Vargas et al.⁸ concluded that a weak C–H···O hydrogen bond between the hydrogen on an α -carbon and a carbonyl oxygen in peptide backbones is strong enough to play an essential role in protein folding. Studies involving C–H···N hydrogen bonds are less prevalent but still numerous.⁹ A recent theoretical study¹⁰ employs the acetylene–ammonia dimer as a prototypical C–H···N hydrogen bond and examines the effect of a wide variety of theoretical methods on the calculated geometry of the complex. Despite this importance, little is known about C–H

hydrogen bonding and its dependence on hybridization of the s and p orbitals of the carbon and on the presence of electron-withdrawing substituents.

It is generally known that C–H bonds with high s character exhibit exceptional acidity, and this explains the fact that acetylenes as a group are among the most acidic of the hydrocarbons.¹¹ This same effect accounts for the relatively high acidity of the C–H bonds on cyclopropane (Cp) rings.¹² A recent study from this laboratory¹³ has characterized hydrogen-bonded complexes of bromocyclopropane (BrCp) with ammonia and trimethylamine and represents the first example of a (substituted) Cp acting as a proton donor and only the second example of an alkane taking part in a C–H···N hydrogen bond. Coordination of the proton adjacent to the Br substituent on the Cp ring to the nitrogen of the base was evidenced by distinct blue shifts of the C–H(Br) bending modes in the infrared spectrum. *Ab initio* calculations yield an essentially linear $BrC-H\cdots NH_3$ hydrogen bond with a C–H···N distance of 2.301 Å and a hydrogen-bond energy of 2.35 kcal/mol. Further work involving halogen-substituted derivatives of cyclopropane and cyclopentadiene is currently underway in this laboratory.

Matrix isolation, combined with infrared spectroscopy, is ideal for the study of weakly bound complexes.^{14–18} In general, hydrogen-bond formation manifests itself as a distinct shift, broadening, and intensification of the proton donor (hydrocarbon) stretching and bending modes. The nitrogen bases are ideal for such studies because they are much more likely to act as Lewis bases that interact through their lone-pair electrons than to donate a proton.^{19,20} Little work has been done with non-hydrogen donor moieties that act as bases and thus enable the study of hydrocarbons as weak carbon acids. This study was undertaken to characterize the complexes formed when cyclopentadiene (Cpd) was co-deposited with the nitrogen bases ammonia and trimethylamine and the oxygen base dimethyl

* Corresponding author: e-mail samet@dickinson.edu.

ether in argon and nitrogen matrices. As the prototypical cyclic diene, Cpd is interesting in its own right from both experimental and theoretical standpoints. The stability of the Cpd anion is a cornerstone in organic and organometallic chemistry and, like benzene, validates the Huckel $4n + 2$ rule.²¹ It is ideal for this study as it is a stronger acid than most carbon acids (its pK_a is about 15, close to the value for acetylene, which is 16^{21,22}) and its acidic proton is coordinated to an sp^3 -hybridized carbon.

This study will allow a comparison with previous work involving CH hydrogen bonding and represents the first matrix isolation study involving Cpd with nitrogen and oxygen bases. In addition, to our knowledge, the C–H \cdots N(O) hydrogen bond formed between Cpd and the nitrogen and oxygen bases employed here is the first to incorporate a proton on an sp^3 -hybridized carbon that is not adjacent to an electron-withdrawing functional group.

Experimental Section

All of the experiments conducted in this study were carried out in a completely stainless steel vacuum system, with Nupro Teflon-seat high vacuum valves. Pumping was provided by a Model 1400B Welch vacuum pump, and a Varian HSA diffusion pump, with a liquid nitrogen trap. Vacuums on the order of 10^{-7} mm at the gauge (cold cathode, Varian) were attained by use of this apparatus. Cryogenics were supplied by a Model 22 closed-cycle helium refrigerator (CTI, Inc.), which operates down to 10 K. Gas samples were deposited from 2-L stainless steel vessels through a precise metering valve onto the cold surface, which is a CsI window mounted with indium gaskets to a copper block, which is in turn mounted with indium gaskets on the second stage of the CTI Cryogenics refrigerator's cold head. Deposition of the gas samples was perpendicular to the cold surface. Temperatures at the second stage of the cold head were controlled and monitored by an RMC–Cryosystems Model 4025 digital cryogenic temperature controller. The vacuum vessel was equipped with CsI windows and sat in the sample beam of a Nicolet Magna-IR 750 infrared spectrometer for the duration of the experiment, and the sample was monitored during the entire deposition. The matrix isolation apparatus described here is standard and has been described thoroughly elsewhere in the literature.²³

The gaseous reagents employed were NH_3 , $(CH_3)_3N$, and $(CH_3)_2O$ (all Matheson). These reagents were subjected to one or more freeze–thaw cycles at 77 K prior to sample preparation. Cpd was prepared by cracking the dimer²⁴ (dicyclopentadiene, Aldrich, 95% purity) and its purity was checked by low-resolution Fourier transform infrared spectroscopy (FTIR) as well as NMR. The resulting monomer was subjected to several freeze–thaw cycles. Argon and nitrogen (Matheson) were used without further purification as matrix gases.

Samples were deposited in both the single-jet mode and twin-jet mode. In the single-jet mode, the hydrocarbon and base were premixed in a single vacuum manifold and diluted with argon, while in the twin-jet mode the two reactants were co-deposited from separate vacuum lines. Samples were deposited at rates ranging from approximately 0.5 to 2 mmol/h, for times ranging from 22 to 30 h, and at temperatures ranging from 10 to 20 K. Survey scans and high-resolution scans were recorded at resolutions of 0.5, 0.25, and 0.125 cm^{-1} . Some samples were annealed to approximately 32 K and recooled to 16 K, and additional spectra were obtained.

Computational Methods.

Gaussian-98²⁵ was used for all ab initio calculations. To locate the global minimum of the Cpd \cdot NH $_3$ complex, fully uncon-

strained geometry optimizations were conducted at the HF/6-311G+(d,p) level of calculation. On the basis of the electrostatic moments of Cpd, two initial starting geometries were selected: (1) collinear alkyl CH \cdots N and (2) the NH $_3$ lone pair directed toward the vector bisecting the Cpd CH $_2$ group. In both cases, the same minimum geometry was generated, with NH $_3$ located toward the back of the CH $_2$ group, above the Cpd ring, yielding C_s symmetry. Notably, this geometry facilitated NH interaction with the π -electron density of the Cpd ring, in addition to the alkyl CH \cdots N interaction. The HF/6-311G+(d,p) minimum geometry was refined with full HF/6-311G+(d,p) and MP2/6-311G+(d,p) optimizations.²⁶ Normal modes of NH $_3$, Cpd, and the Cpd \cdot NH $_3$ complex were also computed at both HF/6-311G+(d,p) and MP2/6-311G+(d,p) levels of calculation. The interaction energy of the complex, $\Delta E_{int} = (E_{cpd} + E_{NH_3}) - E_{complex}$, was computed by the counterpoise method²⁷ to correct for basis set superposition error.

Results

Prior to any co-deposition studies, blank experiments were carried out on each of the bases employed here. The resulting spectra were in excellent agreement with literature spectra^{28–36} as well as with spectra recorded previously in this laboratory. Our blank cyclopentadiene experiments were in excellent agreement with vapor-phase vibrational studies^{37,38} as well as a matrix isolation study³⁹ involving the cyclopentadiene/iron system. Since band assignments were straightforward, isotopic substitution was not deemed necessary. In addition, since small changes from parent to complex were anticipated, blank experiments were performed whenever a new sample was prepared. This ensured a precise comparison between parent and complex spectra for every concentration of reactants studied. Once it was established that single-jet results did not provide any additional information, all experiments were performed in the twin-jet mode. All of the results provided here are from twin-jet depositions. Deposition window temperature as well as reactant flow rates were varied in these experiments so that optimal conditions for maximum product formation could be determined. In all experiments, band positions were reproducible within ± 0.2 cm^{-1} . Representative spectra for the systems described below are shown in Figures 1–5.

Cpd + NH $_3$. Cpd/Ar and NH $_3$ /Ar were co-deposited in many experiments at concentrations ranging from 1000/1/1 (Ar/Cpd/NH $_3$, meaning Ar/Cpd at 500/1 was co-deposited with Ar/NH $_3$ at 500/1) to 200/1/1. The following new spectral features were observed in all experiments and are summarized in Table 1. In the parent CH $_2$ stretching region, two new absorptions were noted. The first, at 2905.9 cm^{-1} , appeared to the red of the parent antisymmetric (B_2) stretches at 2916.0 and 2909.2 cm^{-1} . The second, at 2891.1 cm^{-1} , appeared to the red of the parent symmetric (A_1) stretches at 2898.6 and 2893.9 cm^{-1} . In the region of the parent CH $_2$ rock, there was a new product absorption at 896.0 cm^{-1} , which appeared as a distinct shoulder to the blue of the parent band at 894.0 cm^{-1} . Close to the CH $_2$ rock, there was a slight increase in intensity of a parent CH bending mode at 917.7 cm^{-1} and a dramatic increase in a parent ring mode at 914.3 cm^{-1} . There was a new absorption at 1243.4 cm^{-1} , about 3 cm^{-1} to the blue of a parent band at 1240.1 cm^{-1} , which is predominantly CH bending and ring stretching. In addition, there were intensity changes in two other CH bending and ring stretching modes at 959.4 and 1294.5 cm^{-1} . In the CH stretching region, two new absorptions were noted. The first, at 3053.6 cm^{-1} , fell between parent bands at 3057.2 and 3049.5 cm^{-1} , which belong to a doublet. The second, at 3046.5 cm^{-1} ,

TABLE 1: Observed and Calculated Vibrational Frequencies Associated with the Cyclopentadiene Fundamentals^a

observed		fundamental ^b	calculated ^a		
Cpd	Cpd·NH ₃		Cpd	Cpd·NH ₃	collinear CH···N
3117.0 ^c	3117.4 (+0.4)	CH stretching (B ₁ /3105)	3256.1	3254.5 (−1.6)	3251.6 (−4.5)
3100.8	3100.4 (−0.4)	CH stretching (A ₁ /3091)	3263.1	3261.1 (−2.0)	3259.0 (−4.1)
3084.6 ^c	3084.6 (0) ^{c,d}	CH stretching (A ₁ /3075)	3238.7	3236.6 (−2.1)	3234.1 (−4.6)
3053.4 ^c	3050.0 ^c (−3.4)	CH stretching (B ₁ /3043)	3229.9	3227.4 (−2.5)	3225.2 (−4.7)
2912.6 ^c	2905.9 (−6.7)	CH ₂ antisymmetric stretch (B ₂ /2900)	3109.2	3115.2 (+6.0)	3097.9 (−11.3)
2896.3 ^c	2891.1 (−5.2)	CH ₂ symmetric stretch (A ₁ /2886)	3064.5	3065.8 (+1.3)	3048.2 (−16.3)
1294.5 ^e	1294.5 (0) ^d	CH bend and ring stretch (B ₁ /1292)	1321.4	1322.3 (+0.9)	1324.6 (+3.2)
1240.1	1243.4 (+3.3)	CH bend and ring stretch (B ₁ /1239)	1270.2	1274.1 (+3.9)	1287.7 (+17.5)
959.4 ^e	958.4 (0) ^d	CH bend and ring stretch (B ₁ /959)	989.6	992.8 (+3.2)	998.9 (+9.3)
894.0	896.0 (+2.0)	CH ₂ rocking (B ₂ /891)	911.0	910.6 (−0.4)	914.0 (+3.0)
914.3	914.3 (0) ^d	ring (A ₁ /915)	945.3	944.8 (−0.5)	945.6 (+0.3)
917.7	917.7 (0) ^d	CH bending (B ₂ /925)	920.7	926.3 (+5.6)	917.8 (−2.9)
663.8	663.8 (0)	CH bending in-phase (B ₂ /664)	665.3	668.7 (+3.4)	667.3 (+2.0)
		CH bending (A ₂ /700), not allowed	683.1	690.2 (+7.1)	683.4 (+0.3)

^a Frequencies are given as wavenumbers (reciprocal centimeters). Values in parentheses represent the frequency shifts of Cpd·NH₃ with respect to isolated Cpd. Unscaled harmonic frequencies were calculated at the MP2/6-311+G(d, p) level. The Cpd·NH₃ calculations correspond to the global minimum as well as the minimum geometry with a collinear CH···N constraint. ^b Reported liquid-phase values were taken from ref 37, including normal mode and symmetry assignments. ^c Doublet; mean value reported. ^d No shift but increased intensity. ^e Multiplet; mean value reported.

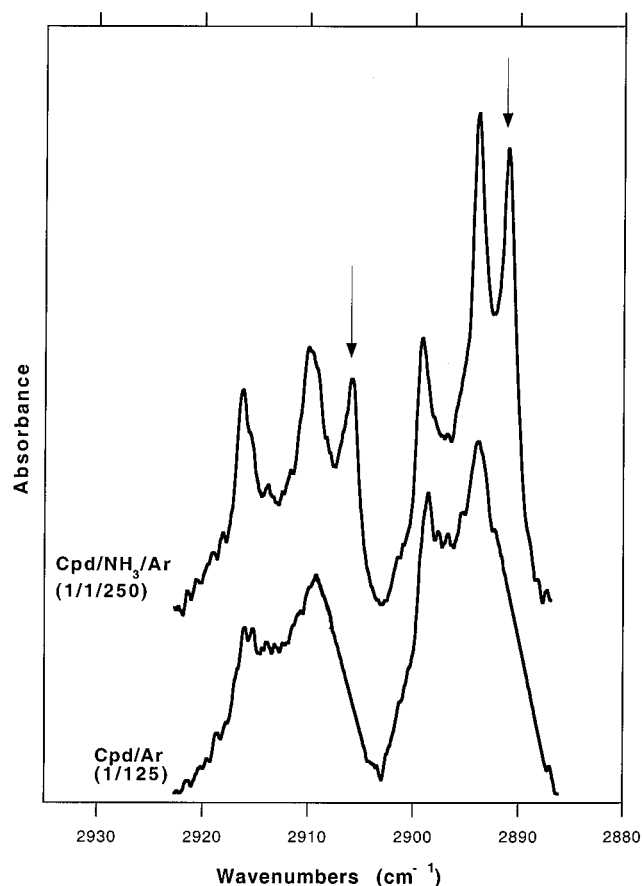


Figure 1. Infrared spectra (0.125 cm^{−1} resolution) in the CH₂ stretching region for parent Cpd/Ar and co-deposition mixture Cpd/NH₃/Ar deposited on CsI at 16 K. New product absorptions are marked with arrows. There are no parent NH₃ absorptions in this region.

fell to the red of this doublet. We note that there were changes in intensity in the three other parent CH stretches. In addition to the perturbations of Cpd fundamental vibrations, we observed new features associated with combination bands involving CH bending modes. Specifically, there was a new product band at 1612.3 cm^{−1}, to the blue of a parent combination band at 1624.5 cm^{−1} (925 + 700). There was also a new product band at 1589.8 cm^{−1}, to the red of a combination band at 1593.2 cm^{−1} (925 +

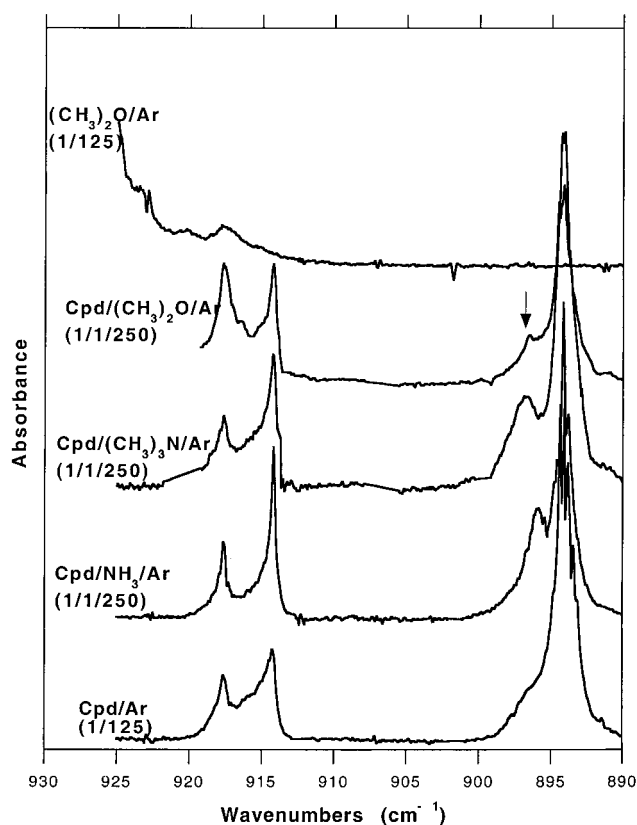


Figure 2. Infrared spectra (0.125 cm^{−1} resolution) in the region of the CH₂ rock for parent Cpd/Ar and co-deposition mixtures deposited on CsI at 16 K. The new product absorption is marked with an arrow. There are no parent NH₃ or (CH₃)₃N absorptions in this region, and the slight (CH₃)₂O absorption is shown in the uppermost trace.

664). We note that these combination bands, which are very weak in the parent spectra, showed a notable increase in intensity upon complex formation. Finally, in all experiments, new bands were observed at 3320.1 and 3232.4 cm^{−1}, near the N–H stretching mode. In addition, several parent bands in this region were slightly shifted. Since NH₃ undergoes hindered rotation in argon matrices³⁵ but not in nitrogen matrices,⁴⁰ several experiments were performed in which Cpd/N₂ and NH₃/N₂ were co-deposited in an attempt to clarify the spectral regions near

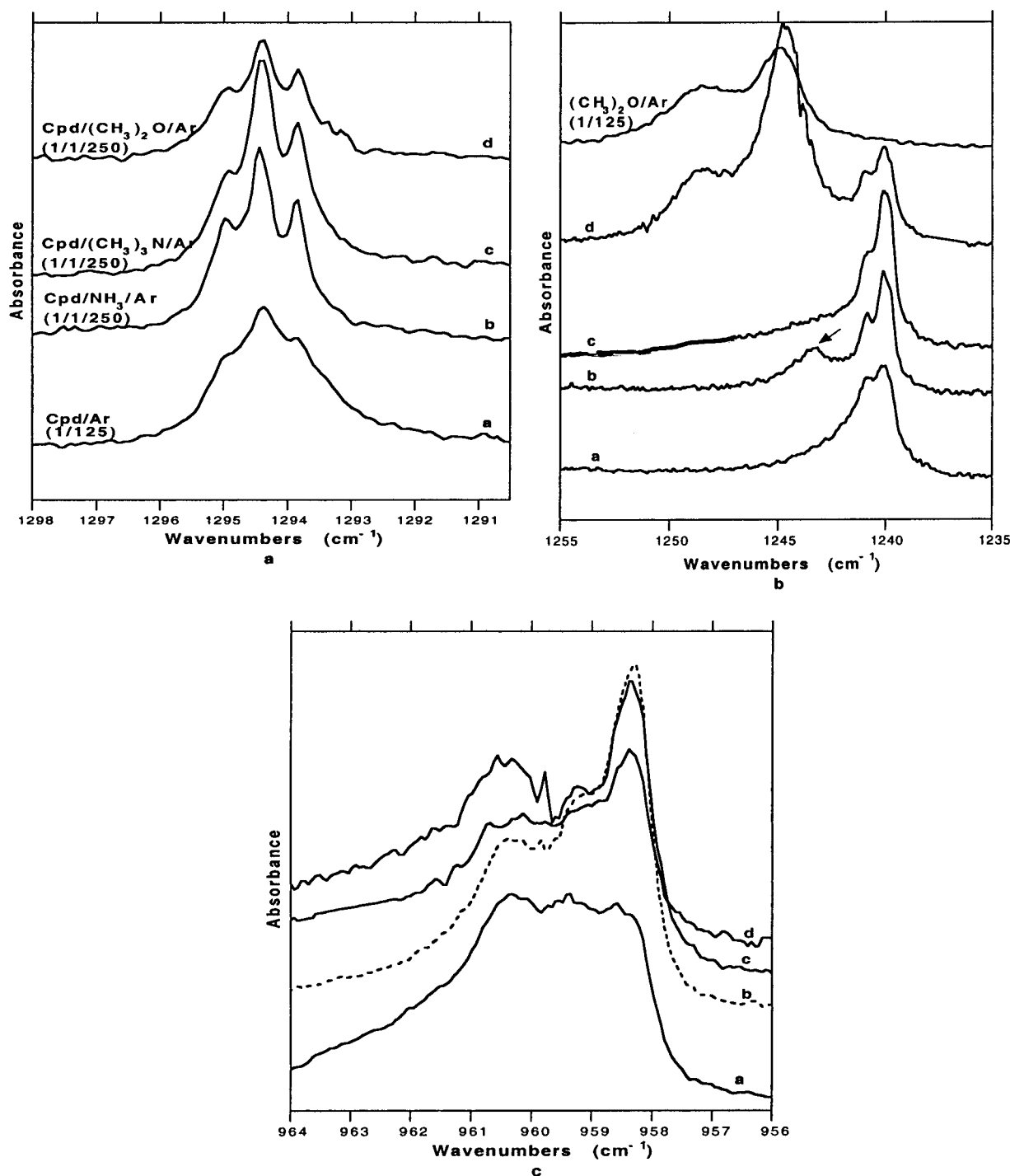


Figure 3. Infrared spectra (0.125 cm^{-1} resolution) in three different CH bending and ring stretching regions (panels a–c) for parent Cpd/Ar (trace a) and co-deposition mixtures (traces b–d) deposited on CsI at 16 K. There are no parent base absorptions except for the region shown in panel b.

NH_3 fundamentals. The results in nitrogen matrices were similar in terms of cyclopentadiene fundamentals, although argon matrices gave much sharper, more definitive spectra. Also, there was more overlap between parent cyclopentadiene modes and base modes than in the argon matrices and therefore new spectral features were not as convenient to study. The nitrogen experiments yielded no new information in the region of the symmetric deformation or “umbrella” mode of NH_3 .

Cpd + $(\text{CH}_3)_3\text{N}$. Co-deposition of Cpd/Ar with $(\text{CH}_3)_3\text{N}$ /Ar at a wide range of concentrations led to spectral features that were essentially identical to those described above for Cpd/Ar with NH_3 /Ar with the following exceptions. The CH_2 stretching region overlapped with parent $(\text{CH}_3)_3\text{N}$ bands, and the region

was not as clear as with NH_3 and was therefore difficult to study. The product band to the blue of the parent CH_2 rock appeared at 896.7 cm^{-1} and was broader than with NH_3 . We did not observe a new absorption to the blue of the parent CH bending and ring stretching mode at 1240.1 cm^{-1} . In the CH stretching region, there were no new absorptions. Finally, slight shifts in parent base modes between 1272 and 1265 cm^{-1} were noted. This is the region assigned to a mode (1272 cm^{-1}) that is predominantly skeletal stretching with some CH_3 rocking character.

Cpd + $(\text{CH}_3)_2\text{O}$. Co-deposition of Cpd/Ar with $(\text{CH}_3)_2\text{O}$ /Ar at a wide range of concentrations led to spectral features that were essentially identical to those described above for Cpd/

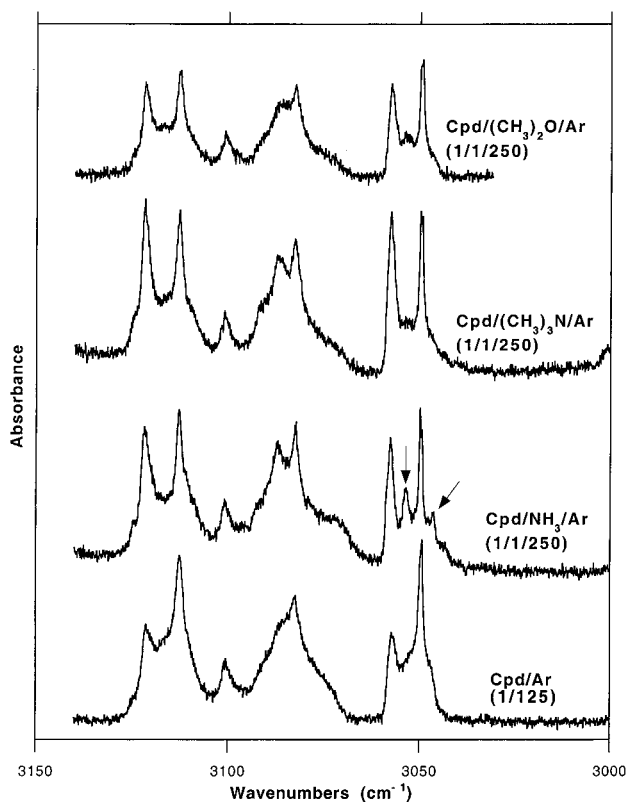


Figure 4. Infrared spectra (0.125 cm^{-1} resolution) in the CH stretching region for parent CpD/Ar and co-deposition mixtures deposited on CsI at 16 K. New product absorptions are marked with arrows. There are no parent base absorptions in this region.

Ar with NH_3/Ar with the following exceptions. As with $(\text{CH}_3)_3\text{N}$, the CH_2 stretching region overlapped with parent $(\text{CH}_3)_2\text{O}$ bands and therefore the region was not as clear as with NH_3 and was difficult to study. The product band to the blue of the parent CH_2 rock appeared at 896.5 cm^{-1} and was less distinct than with NH_3 and $(\text{CH}_3)_3\text{N}$. The new product absorption to the blue of the parent CH bending and ring stretching mode at 1240.1 cm^{-1} appeared at 1244.8 cm^{-1} . We note that a $(\text{CH}_3)_2\text{O}$ absorption overlapped with this new product band, but the intensity of this band was so large that it was obvious by subtraction that this was a new product band. Again, we did not observe any new absorptions in the CH stretching region. Finally, two new bands were observed at 1092.9 and 1090.9 cm^{-1} , near the antisymmetric C—O—C stretching mode of the base. In addition, a very weak feature was noted at 923.4 cm^{-1} , near the C—O—C symmetric stretch.

Computational Results.

On the basis of MP2/6-311G+(d,p) ab initio calculations, the minimum geometry of the $\text{CpD}\cdot\text{NH}_3$ complex consists of NH_3 located above the CpD ring, oriented by the weak $\text{C}_\alpha\text{H}\cdots\text{N}$ interaction, as well as coupling between NH and the π -electron density of the CpD ring. The complex has C_s symmetry. The global minimum geometry is given in Figure 6. Notably, the $\text{C}_\alpha\text{H}\cdots\text{N}$ distance (2.74 \AA) is similar to the $\text{NH}\cdots\text{C}_\beta$ (2.80 \AA) and $\text{NH}\cdots\text{C}_\gamma$ (2.77 \AA) distances. On average, these distances increase by 16% at the Hartree–Fock HF/6-311G+(d,p) level of calculation, indicating the importance of electron correlation to a stronger $\text{CpD}\cdot\text{NH}_3$ interaction. The calculated MP2 interaction energy (ΔE_{int}) of the complex was 2.40 kcal/mol . In comparison, the HF interaction energy was substantially weaker, $\Delta E_{\text{int}} = 0.97\text{ kcal/mol}$. The $\text{CpD}\cdot\text{NH}_3$ complex was also minimized with the $\text{C}_\alpha\text{H}\cdots\text{N}$ interaction constrained to be

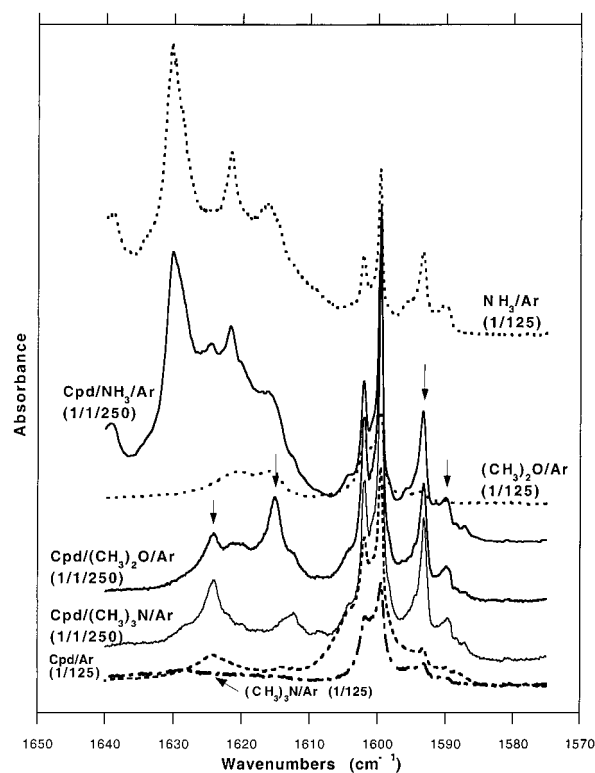


Figure 5. Infrared spectra (0.125 cm^{-1} resolution) in the region of the CH bending combination bands for parents CpD/Ar, NH_3/Ar , $(\text{CH}_3)_3\text{N}/\text{Ar}$, and $(\text{CH}_3)_2\text{O}/\text{Ar}$ (broken lines) and co-deposition mixtures (solid lines) deposited on CsI at 16 K. New product absorptions are marked with an arrow.

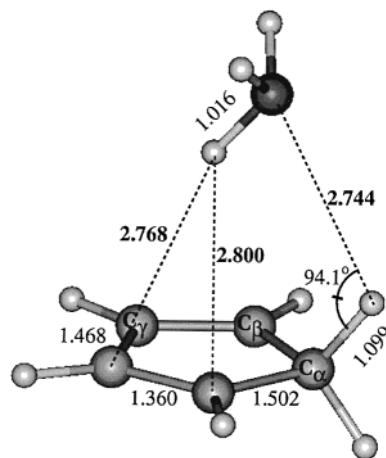


Figure 6. MP2/6-311G+(d,p) minimum geometry of the $\text{CpD}\cdot\text{NH}_3$ complex (C_s symmetry).

collinear. The MP2/6-311G+(d,p) $\text{C}_\alpha\text{H}\cdots\text{N}$ distance under this constraint was 2.478 \AA , and the MP2 interaction energy of the complex was 1.27 kcal/mol . Given the results above, this suggests that approximately half of the interaction energy of the global minimum is derived from the $\text{C}_\alpha\text{H}\cdots\text{N}$ interaction and half from NH interaction with the CpD π -density.

Harmonic frequencies for isolated CpD, NH_3 , and $\text{CpD}\cdot\text{NH}_3$ were calculated at the MP2/6-311G+(d,p) level. Frequency shifts in the CpD normal modes, due to formation of $\text{CpD}\cdot\text{NH}_3$, are compared with experimental observations in Table 1. In addition to the global minimum results, frequency shifts of the constrained collinear $\text{C}_\alpha\text{H}\cdots\text{N}$ complex are also included. Since only relative frequency shifts are of interest, unscaled ab initio frequencies are reported.

Discussion

Evidence for an interaction between Cpd and the bases comes from a direct comparison of the infrared spectra of the isolated hydrocarbon acid and bases (i.e., the blank or parent spectra) with those spectra obtained in the co-deposition experiments. In the co-deposition experiments, new absorptions were noted that could not be ascribed to either parent species. These spectral changes are consistent with those that are known to occur as a result of hydrogen-bond formation.^{14–18} Furthermore, the distinctness and intensity of the product bands supports the idea that the interaction is specific and directional rather than nondirectional and dispersive (van der Waals). The observed product bands can be grouped into three general sets: (1) those occurring near parent modes that significantly displace the CH₂ group, (2) those appearing near olefinic CH stretching and bending modes, and (3) those occurring near vibrational modes of the base. The nearness of the product absorptions to modes of the parent species suggests that the Cpd and bases retain their structural integrity and therefore the product is not the result of addition, elimination, or rearrangement of the subunits. The fact that the product bands were observed over the entire range of reagent concentrations and the intensities of these product absorptions were directly proportional to the concentration of the reagents points to a single product species with 1:1 stoichiometry. Our annealing studies also support this conclusion. We note that although all of the new spectral features were observed over the entire range of concentrations, product yields were best and spectral features most clear when the Cpd/base/Ar ratio was 1/1/250.

The observable most commonly used in the characterization of hydrogen-bonded systems is the shift of the parent C–H stretch that involves the hydrogen-bonded hydrogen. Previous work involving alkynes^{14–16} and alkenes^{17,18} confirms that this shift, usually referred to as $\Delta\nu_s$, is a reliable measure of the strength of interaction. For Cpd, both CH₂ stretching modes are infrared-active. These modes involve the hydrogen-bonded hydrogen, and therefore perturbations in these modes should be indicative of interaction strength. When Cpd was co-deposited with NH₃, two new absorptions were observed near and to the red of the parent CH₂ symmetric and antisymmetric stretches (see Figure 1). In the Cpd/NH₃ experiments, these bands are easy to study, since there are no NH₃ absorptions in this region. With (CH₃)₃N and (CH₃)₂O, there are base modes in this region that are very intense and make subtraction spectra difficult to obtain. In argon matrices, both parent CH₂ stretches occur as a doublet. The doublet structure in the parent CH₂ stretches could result from slightly different packing sites within the argon matrix, as is common in matrix experiments.⁴¹ If we take the mean value of each doublet and calculate the shift from parent to complex, then, one of the bands lies about 7 cm^{−1} to the red of the parent CH₂ antisymmetric stretch and the second lies about 5 cm^{−1} to the red of the parent CH₂ symmetric stretch. These shifts are the largest observed in the co-deposition spectra. Our shift of 7 cm^{−1} in the antisymmetric stretch is much smaller than what Ault reports for alkynes (30–300 cm^{−1}) but close to the lower limit of what he reports for alkenes (10–150 cm^{−1}).^{14–18} In our previous bromocyclopropane–NH₃ work, the shift in ν_s fell within the envelope of parent absorptions but was calculated to be 6.9 cm^{−1}.¹³

Another characteristic spectral change upon hydrogen-bond formation is a shift to higher energy of the proton donor bending modes, with shifts that in general are smaller than $\Delta\nu_s$. The third new product band involving a CH₂ mode lies 2.0 cm^{−1} to the blue of the parent CH₂ rocking mode at 894.0 cm^{−1} (see

TABLE 2: Calculated Vibrational Frequencies^a for Cyclopentadiene Fundamentals^b

fundamental (symmetry/lit. value ^c)	Cpd	Cpd·NH ₃	collinear C–H···N
CH ₂ scissor (A ₁ /1378)	1425.7	1420.9 (−4.8)	1437.9 (+12.2)
CH ₂ twist (A ₂ /1135), not allowed	1111.2	1121.6 (+10.4)	1140.2 (+29.0)
CH ₂ wag (B ₁ /1090)	1109.7	1108.0 (−1.7)	1107.1 (−2.6)
ring (B ₂ /350)	314.0	323.9 (+9.9)	351.3 (+37.3)
ring (B ₁ /805)	810.1	812.2 (+2.1)	812.1 (+2.0)
ring bend (A ₂ /515)	493.6	502.9 (+9.3)	500.6 (+7.0)
C=C stretch (B ₁ /1580)	1608.6	1602.7 (−5.9)	1604.8 (−3.8)
C=C stretch (A ₁ /1500)	1532.8	1526.7 (−6.1)	1528.6 (−4.2)

^a Frequencies are given as wavenumbers (reciprocal centimeters). Values in parentheses represent the frequency shifts of Cpd·NH₃ with respect to isolated Cpd. Unscaled harmonic frequencies were calculated at the MP2/6-311+G(d, p) level. The Cpd·NH₃ calculations correspond to the global minimum as well as the minimum geometry with a collinear CH···N constraint. ^b These are all fundamentals that show no experimental changes upon complex formation. ^c Reported liquid-phase values were taken from ref 37, including normal mode and symmetry assignments.

Figure 2). There are no base absorptions in this region [except for a slight (CH₃)₂O absorption, which falls under the Cpd parent band at 917.7 cm^{−1}] and we observe a product band with all three bases. The CH₂ rock can be considered to be analogous to proton donor bending modes. Our shift of 2 cm^{−1} is smaller than what Ault reports for alkynes and alkenes.^{14–18} Previous work from this laboratory shows that coordination of the acidic proton of bromocyclopropane to the nitrogen of NH₃ and (CH₃)₃N was evidenced by distinct blue shifts of the C–H(Br) bending modes, with shifts (~12 cm^{−1} for the in-plane bend and ~6 cm^{−1} for the out-of-plane bend) that are much smaller than for alkenes and alkynes.¹³ In addition to the rocking mode, there are CH₂ scissoring (sometimes referred to as bending), twisting (infrared inactive), and wagging modes for Cpd. These parent bands are very weak and we observe no changes upon complex formation. Although all of these modes are predicted to shift upon complex formation (see Table 2), the product bands are calculated to have almost zero intensity.

Additional modes of the Cpd were perturbed by hydrogen-bond formation (see Figure 3). Upon coordination of the nitrogen of the base to the acidic hydrogen of Cpd, we would expect to see perturbations in Cpd modes that involve the CH₂ group. More specifically, if the CH₂ group moves during a vibration, then this vibration would also be affected by hydrogen-bond formation. Experimentally, we observe a new product band near and to the blue of a parent CH bending and ring stretching mode at 1240.1 cm^{−1}. This band appears 3.3 cm^{−1} to the blue of the parent band with NH₃ and 4.7 cm^{−1} to the blue of the parent mode with (CH₃)₂O. We do not observe a new product band with (CH₃)₃N, but we suspect that it falls underneath the parent absorption. On the basis of molecular mechanics and ab initio results, all three CH bending and ring stretching modes cause significant displacement of the CH₂ protons of Cpd. Notably, two of these modes with the largest calculated shifts displace the CH₂ protons as much as the CH₂ stretch and rock modes.

In addition to the modes discussed above, we observe changes in CH stretching modes and combination bands involving CH bending. Specifically, there are four parent modes in the CH stretching region (see Figure 4), and two of them (B₁, 3105 cm^{−1}, and B₁, 3043 cm^{−1}) are split into doublets in the argon matrix. A third (A₁, 3075 cm^{−1}) shows a hint of a shoulder, and the fourth (A₁, 3091 cm^{−1}, the in-phase stretch) remains a singlet. The new product band at 3053.6 cm^{−1} is assigned to the B₁ mode since it appears in the middle of the doublet. The

other new band appears just to the red of this doublet. It is likely that this B_1 doublet is red-shifted by about 4 cm^{-1} from the parent doublet since there is the same distance between peaks in both parent and complex doublets. We note that although we observe intensity changes in some of the CH stretches with $(\text{CH}_3)_3\text{N}$ and $(\text{CH}_3)_2\text{O}$, we do not observe any new product bands with these bases. We emphasize that these four CH stretches do not displace the CH_2 group. In addition, we observe new features associated with combination bands that involve CH bending (see Figure 5). In particular, we observe a weak new feature about 12 cm^{-1} to the red of a combination band at 1624.5 cm^{-1} as well as a new product band about 3 cm^{-1} to the red of a second combination band at 1593.2 cm^{-1} . These two combination bands arise from the addition of a CH bend at 925 cm^{-1} with those at 664 (the in-phase bend) and 700 cm^{-1} , respectively.³⁷ We note that we do not observe significant changes in these parent modes. The mode at 925 cm^{-1} is predicted to blue-shift but to be of almost zero intensity. The in-phase CH bending mode is very broad and intense in the matrix, and it is likely that the shift falls within the envelope of the parent absorption. This mode is predicted to shift by $2\text{--}3\text{ cm}^{-1}$, thus supporting the lack of observation of this feature. The third CH bend (700 cm^{-1}) contributing to the combination bands is of A_2 symmetry and is not allowed for Cpd. It is predicted to blue-shift but to be of almost zero intensity. We note that these CH bending modes displace the CH_2 group very slightly.

In general, the $\text{Cpd}\cdot\text{NH}_3$ spectral features are the most clear and distinct of the three bases. In part, this is because the new product bands associated with Cpd fundamentals do not overlap with any NH_3 parent fundamentals. In complexes with stronger hydrogen bonds, systematic trends are observed for a given hydrocarbon through a range of bases, with shifts being larger the stronger the base. In the case of bromocyclopropane, the $(\text{CH}_3)_2\text{O}$ was not a strong enough base to form a complex whereas the nitrogen bases NH_3 and $(\text{CH}_3)_3\text{N}$ were. This makes sense, since nitrogen bases are stronger than oxygen bases.⁴² For $\text{BrCp}\cdot\text{NH}_3$ and $\text{BrCp}\cdot(\text{CH}_3)_3\text{N}$, the shift of the product bands [in-plane and out-of-plane $\text{C}\text{--}\text{H}(\text{Br})$ bending modes] is larger the stronger the base; however, the difference is about 0.5 cm^{-1} , which is quite small.¹³ The differences in shifts with Cpd and the bases is also very small and not systematic, perhaps further supporting the conclusion that this $\text{C}\text{--}\text{H}\cdots\text{N}(\text{O})$ hydrogen bond is weaker than those that incorporate an sp - or sp^2 -hybridized carbon and more on the order of that formed between BrCp and the nitrogen bases. With each base employed, perturbations of base modes were noted. Two new bands were observed in the region of the $\text{N}\text{--}\text{H}$ stretching mode of NH_3 , which is what Ault observed with the alkynes C_2H_2 and C_3H_4 .¹⁵ Our calculations predict a red shift of 2.4 cm^{-1} in this mode. A small shift was noted in the CH_3 rocking mode of $(\text{CH}_3)_3\text{N}$. It is interesting to note that Ault does not report any new product bands near vibrational modes of $(\text{CH}_3)_3\text{N}$ with C_2H_2 and C_3H_4 . Finally, we observe two new product bands of medium intensity near the $\text{C}\text{--}\text{O}\text{--}\text{C}$ antisymmetric stretching mode of $(\text{CH}_3)_2\text{O}$ and a very weak band near the $\text{C}\text{--}\text{O}\text{--}\text{C}$ symmetric stretch. Ault reports similar changes in these modes with several substituted alkynes.¹⁶ We did not observe any changes in base modes in the $\text{BrCp}\text{--}\text{base}$ systems.¹³

Structure of the Complex.

Our experimental results suggest that the products described are the isolated 1:1 hydrogen-bonded complex of cyclopentadiene with each base. Although the CH_2 stretching product bands for the $\text{Cpd}\cdot(\text{CH}_3)_3\text{N}$ and $\text{Cpd}\cdot(\text{CH}_3)_2\text{O}$ systems fell underneath

parent base absorptions and were therefore difficult to study, the observation of product bands in other spectral regions supports the observation of these complexes as well. Since cyclopentadiene is a strong acid ($\text{p}K_a\ 15$) compared to other types of alkenes, we would expect a hydrogen-bond interaction to occur between the acidic alkyl proton (CH_2 proton) and the $\text{N}(\text{O})$ of the base, forming a $\text{C}\text{--}\text{H}\cdots\text{N}(\text{O})$ hydrogen bond. This is supported by the new product bands associated with the CH_2 stretches, the CH_2 rock, and the CH bending and ring stretching mode, all of which are modes that displace the CH_2 or alkyl protons. The CH stretching modes, however, do not displace the CH_2 group at all (our calculations predict zero displacement for both hydrogen atoms), and the CH bending modes displace it only slightly. Therefore, these modes would not necessarily be expected to shift upon $\text{C}\text{--}\text{H}\cdots\text{N}$ hydrogen-bond formation. These perturbations, then, provide evidence for an additional interaction between Cpd and the bases. It is very likely that the olefinic CH stretching motions are being perturbed as a result of the protons of ammonia interacting with the π -electron density of Cpd. This type of interaction is well-documented^{43,44} and has been shown to result in shifts of the $\text{C}=\text{C}$ stretching modes as well as CH stretching and bending modes. There are two $\text{C}=\text{C}$ stretching modes for Cpd. The in-phase (A_1) stretch is not observed in our matrix and the out-of-phase (B_1) stretch is very weak, a result also obtained in a previous matrix isolation study of Cpd with Fe atoms.³⁹ These bands, therefore, are not able to provide us with evidence for this $\text{NH}\cdots\pi$ interaction, as is the case for many olefins whose $\text{C}=\text{C}$ stretching fundamental is infrared-inactive. If we consider ethylene as a model for the $\text{C}=\text{C}$ subunit in Cpd, we find evidence to support this $\text{NH}\cdots\pi$ interaction. A previous matrix isolation study shows that water forms a hydrogen bond with ethylene where one of its hydrogen atoms points toward the midpoint of the $\text{C}=\text{C}$ bond.⁴³ Although the $\text{C}=\text{C}$ stretch for ethylene is infrared-inactive, the interaction is evidenced by perturbations in the out-of-plane bending of ethylene (ν_7), which shifts by 12.2 cm^{-1} to higher energy. In addition, a combination band ($\nu_7 + \nu_8$) is blue-shifted by 16.9 cm^{-1} . Another matrix study of larger olefins with water shows that, of the hydrocarbon fundamentals, those involving out-of-plane bends of hydrogens next to the double bond are those most affected by complex formation. For those olefins where the $\text{C}=\text{C}$ bond stretching fundamental is active, it shifts a few wavenumbers to lower energy upon complex formation. These complexes, like ethylene, have the hydrogen of water interacting with the π orbital on the hydrocarbon.⁴⁴ Our ab initio calculations predict red shifts ($4\text{--}6\text{ cm}^{-1}$, see Table 2), for the in-phase and out-of-phase $\text{C}=\text{C}$ stretches but almost zero intensity for both product bands. Although our parent CH bending modes alone do not provide any information (although they are calculated to shift in the complex), the fact that we also observe new absorptions associated with the combination bands that involve these parent CH bends may support this interaction. Finally, we note that the spectrum is similar in this region for all three bases, when in fact NH_3 is the only base capable of such a hydrogen-bonding interaction. There are several explanations for this. For one, these CH bends do slightly displace the alkyl protons, and second, these modes are coupled to the CH_2 rock. Thus, it is likely that perturbations in these modes result from both the $\text{C}\text{--}\text{H}\cdots\text{N}$ and $\text{NH}\cdots\pi$ hydrogen-bonding interactions. Although these ethylene studies do not reveal changes in CH stretching modes, a study of $\text{H} + \text{C}_2\text{H}_4$,⁴⁵ which can also serve as a model for a H atom interacting with an olefin, shows that when the H atom interacts with the ethylene, the CH stretching modes are shifted to lower energy. The electronic

factors that give rise to the lengthening of the CH bonds are also associated with a reduction in the CH stretching force constant. This may further support that the changes we observe in Cpd CH stretching modes result from a similar interaction. The new product bands that we observe in this region are associated with the lower-energy B₁ stretch, and we do not observe these product bands with (CH₃)₃N or (CH₃)₂O. Furthermore, this CH stretch is not coupled to proton donor modes and does not displace the CH₂ protons. Therefore, the only justification for these spectral features is a NH $\cdots\pi$ interaction. We note that although our ab initio calculations predict an approximately equal red shift for all four CH stretching modes, we observe a red shift in the lowest energy B₁ mode only.

The calculated minimum of the Cpd·NH₃ complex (see Figure 6) strongly supports our data. Consistent with ab initio calculations, we see spectral evidence for a C–H \cdots N hydrogen-bonding interaction as well as interaction with the Cpd C=C subunits, as summarized in Table 1. Notably, all perturbations in the observed Cpd parent modes correspond to modes that are calculated to change. For example, of the three CH bending and ring stretching modes, our new product band is associated with the mode that is calculated to have the largest shift. However, the calculated shifts for the CH₂ symmetric and antisymmetric stretches are blue-shifted, contrary to observation. Given that the Cpd·NH₃ complex corresponds to a shallow energy minimum, this result may reflect the sensitivity of the frequency shifts to variation in the Cpd·NH₃ geometry. This was explored by minimizing Cpd·NH₃ under the constraint of a collinear CH \cdots N interaction. In this configuration, the CH₂ symmetric and antisymmetric stretches become red-shifted, consistent with experiment (Table 1). Similarly, agreement with the shift of the CH₂ rock also improves. This finding suggests a population of Cpd·NH₃ configurations may exist in the matrix that vary between a dominant CH \cdots N interaction and a substantial NH $\cdots\pi$ interaction component with the Cpd ring. Perturbation of the Cpd·NH₃ geometry by the matrix remains a further consideration.

There are several modes not yet discussed that are predicted to change for which we do not observe any spectral features (see Table 2). One is a far-infrared ring bending mode at 314.0 cm⁻¹, which is predicted to blue-shift by a large amount but is in a region that we did not study. Another is a ring bending mode that is infrared-inactive and is predicted to shift to higher energy by 7–9 cm⁻¹ but to be of almost zero intensity. Both of these modes significantly displace the CH₂ group. Finally, we emphasize that we did not observe any product bands for which there was not a calculated shift.

Conclusions

This work represents the first detailed matrix isolation study of Cpd with strong bases. New product bands associated with the CH₂ symmetric and antisymmetric stretches and the CH₂ rock provide strong evidence for a C–H \cdots N and C–H \cdots O hydrogen-bonding interaction between Cpd and the bases. These proton donor modes are known indicators of hydrogen-bond formation and provide a measure of interaction strength. Our results confirm that the C–H \cdots N(O) hydrogen bond formed between Cpd and the bases is much weaker than those involving an sp²-hybridized carbon. The new product bands associated with the lowest energy B₁ olefinic CH stretch provide evidence for an additional interaction between the protons of NH₃ and the π -electron density of the Cpd ring. Additional CH stretching and bending modes that might otherwise provide further evidence for this NH $\cdots\pi$ interaction are coupled with CH₂

stretching and rock modes, thereby making it difficult to assign spectral features to a specific interaction. The calculated geometry of the Cpd·NH₃ complex supports these experimental findings. The overall interaction energy of 2.40 kcal/mol demonstrates the weakness of the interaction in these systems. Although there are several examples of weak inter- and intramolecular C–H \cdots O hydrogen bonds between the proton on a carbon that is adjacent to a carbonyl (an α -carbon) and a carbonyl or hydroxyl oxygen, this study presents the first example of an sp³-hybridized carbon that is not adjacent to a carbonyl or other electron-withdrawing substituent forming a C–H \cdots N(O) hydrogen bond.

Acknowledgment. We gratefully acknowledge support of this research by the National Science Foundation through Grant CHE-9501428 (under the Research in Undergraduate Institutions program) and by the Whitaker Foundation under a student–faculty research program administered by Dickinson College. We also thank the staff of the Advanced Biomedical Computing Center for resources and technical support. The computational portion of this project was funded in part with federal funds from the National Cancer Institute, NIH, under Contract NO1-CO-56000. The content of this publication does not necessarily reflect the views or policies of the Department of Health and Human Services, nor does mention of trade names, commercial products, or organizations imply endorsement by the U.S. government.

References and Notes

- (1) Pimentel, G. C.; McClellan, A. L. *The Hydrogen Bond*; W. H. Freeman: San Francisco, 1960.
- (2) Smith, D. L. *Eng. Sci.* **1994** (Fall), 27.
- (3) Pauling, L. *The Nature of the Chemical Bond and the Structure of Molecules and Crystals: An Introduction to Modern Structural Chemistry*, 3rd ed.; Cornell University Press: Ithaca, NY, 1960; pp 449–504.
- (4) Taylor, R.; Kennard, O. *J. Am. Chem. Soc.* **1982**, *104*, 5063.
- (5) See, for example, Scaccianoc, L.; Braga, D.; Calhorda, M. J.; Grepioni, F.; Johnson, B. F. G. *Organometallics* **2000**, *19*, 790 and references therein.
- (6) Chao, M.; Kumaresan, S.; Wen, Y.; Lin, S.; Hwu, J. R.; Lu, K. *Organometallics* **2000**, *19*, 714.
- (7) Hansen, J. G.; Feeder, N.; Hamilton, D. G.; Gunter, M. J.; Becher, J.; Sanders, J. K. M. *Org. Lett.* **2000**, *2*, 449.
- (8) Vargas, R.; Garza, J.; Dixon, D. A.; Hay, B. P. *J. Am. Chem. Soc.* **2000**, *122*, 4750.
- (9) See, for example, (a) Reddy, D. S.; Goud, B. S.; Panneerselvam, K.; Desiraju, G. R. *J. Chem. Soc., Chem. Commun.* **1993**, 663. (b) Reddy, D. S.; Craig, D. C.; Desiraju, G. R. *J. Am. Chem. Soc.* **1996**, *118*, 4090.
- (10) Hartmann, M.; Radom, L. *J. Phys. Chem. A* **2000**, *104*, 968.
- (11) Bordwell, F. G.; Matthews, W. S. *J. Am. Chem. Soc.* **1974**, *96*, 1214.
- (12) See, for example, Burnett, W. J. *J. Chem. Educ.* **1967**, *44*, 17.
- (13) Bedell, B. L.; Goldfarb, L.; Mysak, E. R.; Samet, C.; Maynard, A. *J. Phys. Chem. A* **1999**, *103*, 4572.
- (14) DeLaat, A. M.; Ault, B. S. *J. Am. Chem. Soc.* **1987**, *109*, 4232.
- (15) Jeng, M. L. H.; DeLaat, A. M.; Ault, B. S. *J. Phys. Chem.* **1989**, *93*, 3997.
- (16) Jeng, M. L. H.; Ault, B. S. *J. Phys. Chem.* **1989**, *93*, 5426.
- (17) Jeng, M. L. H.; Ault, B. S. *J. Phys. Chem.* **1990**, *94*, 1323.
- (18) Jeng, M. L. H.; Ault, B. S. *J. Phys. Chem.* **1990**, *94*, 4851.
- (19) Nelson, D. D., Jr.; Fraser, G. T.; Klemperer, W. *Science* **1987**, *238*, 1670.
- (20) Baum, R. M. *Chem. Eng. News* **1992** (Oct. 19), 20.
- (21) Cram, D. J. *Fundamentals of Carbanion Chemistry*; Academic Press: New York, 1965.
- (22) Streitwieser, A.; Caldwell, R. A.; Young, W. R. *J. Am. Chem. Soc.* **1969**, *91*, 529.
- (23) See, for example, Ault, B. S. *J. Am. Chem. Soc.* **1978**, *100*, 2426.
- (24) See, for example, (a) Moffett, R. B. *Organic Syntheses*; Wiley: New York, 1963; Collect. Vol. 4, p 238. (b) Williamson, K. L. *Macroscale and Microscale Organic Experiments*; D. C. Heath and Co.: Lexington, MA, 1989; p 320.
- (25) Gaussian 98, Revision A.6; M. Frisch, G. Trucks, H. Schlegel, P. Gill, B. Johnson, M. Robb, J. Cheeseman, T. Keith, G. Petersson, J.

Montgomery, K. Raghavachari, M. Al-Laham, V. Zakrzewski, J. Ortiz, J. Foresman, J. Cioslowski, B. Stefanov, A. Nanayakkara, M. Challacombe, C. Peng, P. Ayala, W. Chen, M. Wong, J. Andres, E. Replogle, R. Gomperts, R. Martin, D. Fox, J. Binkley, D. Defrees, J. Baker, J. Stewart, M. Head-Gordon, C. Gonzalez, and J. A. Pople; Gaussian, Inc., Pittsburgh, PA, 1998.

(26) Krishnan, R.; Binkley, J.; Seeger, R.; Pople, J. A. *J. Chem. Phys.* **1980**, 72, 650.

(27) Boys, S.; Bernardi, F. *Mol. Phys.* **1970**, 19, 553.

(28) Duncan, J. L.; McKean, D. C. *J. Mol. Spectrosc.* **1968**, 27, 117.

(29) Duncan, J. L.; Burns, G. R. *J. Mol. Spectrosc.* **1969**, 30, 253.

(30) Baker, A. W.; Lord, R. C. *J. Chem. Phys.* **1955**, 23, 1636.

(31) Pimentel, G. C.; Bulanin, M. O.; Thiel, M. V. *J. Chem. Phys.* **1961**, 36, 500.

(32) Goldfarb, T. D.; Khare, B. N. *J. Chem. Phys.* **1967**, 46, 3379.

(33) Suzer, S.; Andrews, L. *J. Chem. Phys.* **1987**, 87, 5131.

(34) Barcelo, J. R.; Bellanata, J. *Spectrochim. Acta* **1956**, 8, 27.

(35) Abouaf-Marguin, L.; Jacox, M. E.; Milligan, D. E. *J. Mol. Spectrosc.* **1977**, 67, 34.

(36) Levin, I. W.; Pearce, R. A. R.; Spiker, R. C., Jr. *J. Chem. Phys.* **1978**, 68, 3471.

(37) Gallinella, E.; Fortunato, B.; Mirone, P. *J. Mol. Spectrosc.* **1967**, 24, 345.

(38) Castellucci, E.; Manzelli, P.; Fortunato, B.; Gallinella, E.; Mirone, P. *Spectrochim. Acta* **1975**, 31A, 451.

(39) Ball, D. W.; Kafafi, Z. H.; Hauge, R. H.; Margrave, J. L. *Inorg. Chem.* **1985**, 24, 3708.

(40) Nelander, B. *Chem. Phys.* **1984**, 87, 283.

(41) Craddock, S.; Hinchliffe, A. *Matrix Isolation*; Cambridge University Press: New York, 1975.

(42) Aue, D. H.; Webb, H. M.; Bowers, M. T. *J. Am. Chem. Soc.* **1976**, 98, 8, 311.

(43) Engdahl, A.; Nelander, B. *Chem. Phys. Lett.* **1985**, 113, 49.

(44) Engdahl, A.; Nelander, B. *J. Phys. Chem.* **1986**, 90, 4982.

(45) Schlegel, H. B. *J. Phys. Chem.* **1982**, 86, 4878.